



Generation of light hydrocarbons through Fischer–Tropsch synthesis: Identification of potentially dominant catalytic pathways via the graph–theoretic method and energetic analysis

Yu-Chuan Lin^{a,1}, L.T. Fan^{a,*}, Shahram Shafie^a, Botond Bertók^b, Ferenc Friedler^b

^a Department of Chemical Engineering, Kansas State University, Manhattan, KS 66506-5102, USA

^b Department of Computer Science, University of Pannonia, Veszprém, Egyetem u. 10 H-8200, Hungary

ARTICLE INFO

Article history:

Received 18 September 2007

Received in revised form 18 December 2008

Accepted 15 January 2009

Available online 23 February 2009

Keywords:

Fischer–Tropsch synthesis

Water–gas shift

Pathway

Graph–theoretic

Energetic analysis

Hydrocarbons

ABSTRACT

The Fischer–Tropsch synthesis (FTS) for the production of widely distributed hydrocarbons through the catalytic hydrogenation of carbon monoxide (CO) has been intensively and extensively explored. This is attributable to its immense theoretical as well as practical importance. Naturally, such exploration would be greatly facilitated if the feasible or dominant catalytic pathways (mechanisms) of FTS can be determined. The stoichiometrically feasible and independent catalytic pathways (IP_i's) of FTS have been exhaustively identified via the rigorous graph–theoretic method based on P-graphs (process graphs). The most extensive set of elementary reactions available, which numbers 26, has yielded 24 IP_i's in less than 1 s on a PC. The plausibly dominant pathways have been selected from the stoichiometrically feasible pathways through the analysis of their activation energies. Naturally, the dominant pathway or pathways need ultimately be discriminated among these plausibly dominant pathways via various means, e.g., in situ spectroscopic measurements of intermediates.

© 2009 Elsevier Ltd. All rights reserved.

1. Introduction

Fischer–Tropsch synthesis (FTS), known since the 1920s (Fischer & Tropsch, 1926a,b), involves mainly the reductive polymerization of CO and H₂ (syngas) to manufacture hydrocarbons with trace amounts of oxygenates (Dry & Hoogendoorn, 1981). It has become ubiquitous due to the soaring price of fossil fuels and the potential to be derived from carbon-neutral biomass (Lin & Huber, 2009). It is, therefore, not surprising that continuous effort has been dedicated to the study of FTS experimentally and/or theoretically (Khodakov, Chu, & Fongarland, 2007; Lox & Froment, 1993a,b; Rados, Al-Dahhan, & Dudukovic, 2003). Nevertheless, the definitive mechanism of FTS apparently remains unknown. At least, two mechanisms have been proposed; one is known as the “carbide” (Fischer & Tropsch, 1926c), and the other, “CO insertion” (Pichler & Schulz, 1970). The water–gas shift (WGS) reaction, however, may proceed simultaneously with FTS, thereby complicating the mechanism of this catalytic reaction (Davis, 2001; Van der Laan & Beenackers, 1999).

Recently, Storsæter, Chen and Holmen (2006) have proposed a novel mechanism for FTS on cobalt catalyst, which comprises elementary reactions in the aforementioned mechanisms as well as those in the mechanism of the WGS reaction. They have analyzed the CO conversion, product distribution, and rate of each elementary reaction on the basis of the microkinetic model derived from their novel mechanism. The results have led to the identification of the rate determining steps for the initiation and chain propagation.

Because of their inordinate complexity, the number of stoichiometrically feasible pathways involved in any mechanism of FTS tends to be vast; however, only a limited number would be energetically favorable. Naturally, the identification of such energetically favorable pathways will immensely facilitate the determination of the dominant pathway, which, in turn, will shed light on the validity of the rate-determining steps reported in an earlier work (Storsæter et al., 2006).

The graph–theoretic methods based on conventional formal graphs have been fairly extensively applied in describing algorithmically the chemical species and the catalytic reaction pathways involving these chemical species (Biggs, Lloyd, & Wilson, 1976; Broadbelt, Stark, & Klein, 1994; Djéga-Mariadassou & Boudart, 2003; Klinke & Broadbelt, 1997; Li et al., 2004; Matheu, Lada, Green, Dean, & Grenda, 2001; Matheu, Green, & Grenda, 2003; Matheu, Dean, Grenda, & Green, 2003). It is worth mentioning that method based on informal graphs, which entails invoking heuristics based on some assumptions and analogy, has also been applied

* Corresponding author at: Department of Chemical Engineering, Kansas State University, 1005 Durland Hall, Manhattan, KS 66506-5102, USA.

Tel.: +1 785 532 4327; fax: +1 785 532 7372.

E-mail address: fan@ksu.edu (L.T. Fan).

¹ Present address: Department of Chemical Engineering, University of Massachusetts, 159 Goessmann Laboratory, Amherst, MA 01003-9303, USA.

(Callaghan et al., 2003; Fishtik & Datta, 2002; Vilekar, Fishtik, & Datta, 2007). Invoking the heuristics, however, renders it impossible to totally automate its implementation: some manual intervention is required (Fan et al., 2007).

The current study focuses on the application of the graph-theoretic method based on P-graphs, which is mathematically rigorous and automatically implementable on a PC (Fan, Bertók, Friedler, & Shafie, 2001, Fan, Bertók, & Friedler, 2002; Imreh, Friedler, & Fan, 1996), in exploring the most comprehensive mechanism, i.e., pathways, of FTS; these pathways are substantially more complex than those identified earlier for other catalytic reactions by the P-graph-based method (Fan et al., 2001, 2007, 2008; Lin et al., 2008). In addition, the dominant pathways among those identified have been discovered via energetic analysis.

2. Methodology

The method is presented herein for exhaustively generating the stoichiometrically feasible pathways. Moreover, the approach is described for identifying energetically favorable pathways among the resultant stoichiometrically feasible pathways.

2.1. Generation of stoichiometrically feasible pathways

The graph-theoretic method based on P-graphs to exhaustively generate stoichiometrically feasible pathways stands on two cornerstones (Appendix A). One is the two sets of axioms, including the six axioms of stoichiometrically feasible pathways, each consisting of plausible elementary reactions, for any given overall reaction, and the seven axioms of combinatorially feasible networks of elementary reactions (Fan et al., 2002, 2005). The other is the unambiguous representation of the networks of pathways by P-graphs, which are directed bipartite graphs. P-graphs comprise horizontal bars, which are the nodes representing elementary-reaction steps, circles, which are the nodes representing active or biochemical species, and directed arcs linking these two types of nodes (Friedler, Tarjan, Huang, & Fan, 1992, 1993; Friedler, Varga, & Fan, 1995).

Table 1

Elementary reactions for Fischer-Tropsch synthesis and their forward and reverse activation energies with 5% deviations on Co/Al₂O₃ catalysts (adapted from Storsæter et al., 2006).

Elementary reactions	$\Delta E_{\text{forward}}$ (kJ/mol)	$\Delta E_{\text{reverse}}$ (kJ/mol)
S ₁ CO* ↔ CO*	0	90.8 ± 4.5
S ₂ H ₂ + 2* ↔ 2H*	11.3 ± 0.6	89.1 ± 4.5
S ₃ CO* + H* ↔ C* + OH*	157.1 ± 7.9	23.7 ± 1.2
S ₄ C* + H* ↔ CH* + *	155.6 ± 7.8	23.3 ± 1.2
S ₅ CH* + H* ↔ CH ₂ * + *	50.5 ± 2.5	102.7 ± 5.1
S ₆ CH ₂ * + H* ↔ CH ₃ * + *	20.7 ± 1.0	109.1 ± 5.5
S ₇ CH ₃ * + H* ↔ CH ₄ + 2*	30.8 ± 1.5	63.9 ± 3.2
S ₈ OH* + H* ↔ H ₂ O* + *	38.6 ± 1.9	89.6 ± 4.5
S ₉ H ₂ O* ↔ H ₂ O + *	70.0 ± 3.5	0
S ₁₀ CO* + H* ↔ CHO* + *	118.9 ± 5.9	0
S ₁₁ CHO* + H* ↔ CH ₂ O* + *	12.0 ± 0.6	84.4 ± 4.2
S ₁₂ CH ₂ O* + H* ↔ CH ₃ O* + *	43.8 ± 2.2	36.8 ± 1.8
S ₁₃ CH ₃ O* + * ↔ CH ₃ * + O*	65.0 ± 3.3	48.1 ± 2.4
S ₁₄ O* + H* ↔ OH* + *	55.4 ± 2.8	28.1 ± 1.4
S ₁₅ CO* + O* ↔ CO ₂ **	67.1 ± 3.4	47.7 ± 2.4
S ₁₆ CO ₂ ** ↔ CO ₂ + 2*	27.7 ± 1.4	0
S ₁₇ CH ₃ * + CH ₂ * ↔ CH ₃ CH ₂ * + *	0	157.2 ± 7.9
S ₁₈ CH ₃ * + CH ₂ O* ↔ CH ₃ CH ₂ O* + *	1.0 ± 0.1	64.6 ± 3.2
S ₁₉ CH ₃ * + CO* ↔ CH ₃ CO* + *	38.0 ± 1.9	18.3 ± 0.9
S ₂₀ CH ₃ CO* + H* ↔ CH ₃ CHO* + *	38.5 ± 1.9	58.2 ± 2.9
S ₂₁ CH ₃ CHO* + H* ↔ CH ₃ CH ₂ O* + *	18.9 ± 0.9	26.1 ± 1.3
S ₂₂ CH ₃ CH ₂ O* + * ↔ CH ₃ CH ₂ * + O*	63.7 ± 3.2	45.9 ± 2.3
S ₂₃ CH ₃ CH ₂ * + H* ↔ CH ₃ CH ₃ **	29.1 ± 1.5	65.9 ± 3.3
S ₂₄ CH ₃ CH ₂ * + 2* ↔ CH ₂ CH ₂ ** + H*	25.1 ± 1.3	10.8 ± 0.5
S ₂₅ CH ₃ CH ₃ ** ↔ C ₂ H ₆ + 2*	32.6 ± 1.6	0
S ₂₆ CH ₂ CH ₂ ** ↔ C ₂ H ₄ + 2*	41.8 ± 2.1	0

The aforementioned axioms and P-graph representation give rise to three highly effective algorithms necessary for synthesizing a stoichiometrically feasible pathway comprising elementary reactions. These three algorithms are RPIMSG for maximal-structure generation, RPISSG for solution-structure (combinatorially feasible pathway) generation, and PBT for feasible pathway generation. These algorithms can be deployed to exhaustively identify catalytic and metabolic pathways for catalyzed chemical and biochemical reactions, respectively (Fan et al., 2002, 2005; Lee et al., 2005; Seo et al., 2001).

Table 1 lists the 26 elementary reactions of the microkinetic model for FTS on cobalt catalysts as well as the forward and reverse activation energy changes of these 26 elementary reactions (Storsæter et al., 2006). To present the rational probability distribution of activation energy, a margin of 5% is assumed for each elementary reaction. Fig. 1 illustrates the P-graph representation of one of the independent pathways, IP₆, which has been identified in the current work.

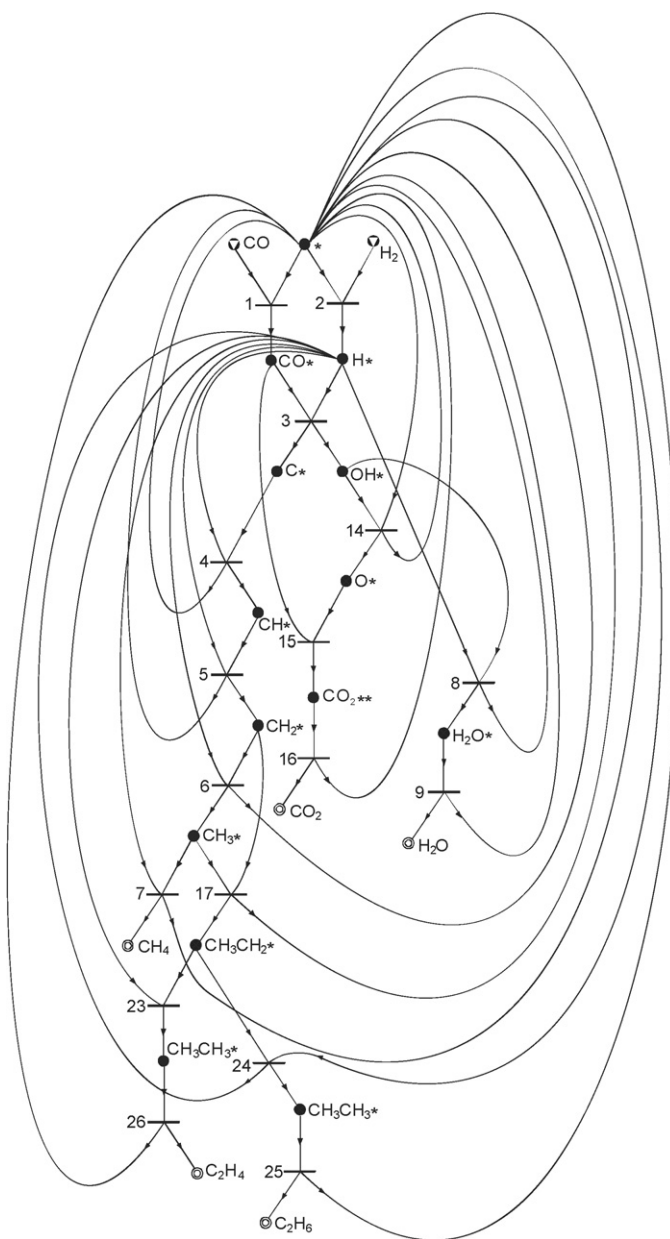


Fig. 1. P-graph representation of independent pathway IP₆.

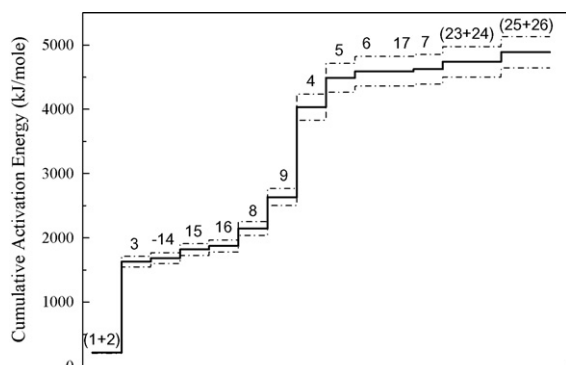


Fig. 2. Activation energy diagram of IP_6 . Note that the 5% deviations assumed are indicated by the dashed-dotted lines.

2.2. Identification of energetically favorable feasible pathways

Energetically favorable feasible pathways are identified by constructing the energetic diagrams of all the stoichiometrically feasible pathways generated. The energetic diagram of each pathway is constructed from the gross activation energies of the elementary reactions constituting this pathway. The gross activation energy of any elementary reaction in the pathway is obtained by multiplying this reaction's activation energy with the corresponding stoichiometric number. The left boundary of the diagram is defined by the sum of the initiation (adsorption) reactions, i.e., CO and H_2 adsorptions. Subsequently, the gross activation energies of successively linked elementary reactions are incorporated into the diagram such that the increase in the cumulative activation energy at each step is as low as possible. The diagram is completed by adding the sum of the gross activation energies of the termination (desorption) reactions, i.e., C_2H_6 and C_2H_4 desorptions, at its right boundary. Fig. 2 plots the activation energy diagram, which yields the cumulative activation energies, of one of the stoichiometrically feasible pathways, i.e., IP_6 , for illustration.

3. Results and discussion

The results obtained are summarized in Table 2 and exhibited in Fig. 3. Table 2 lists the 24 stoichiometrically feasi-

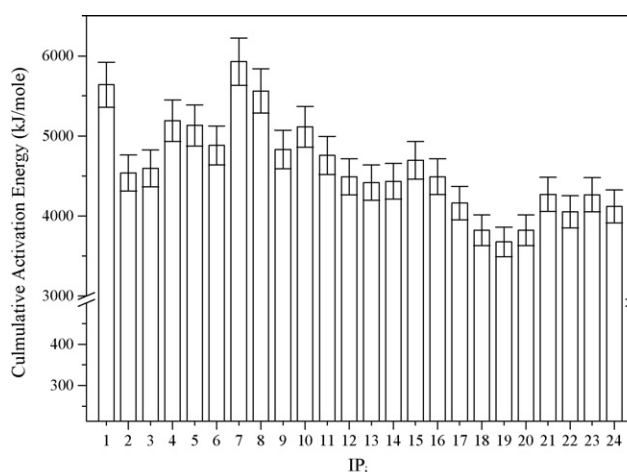


Fig. 3. Cumulative activation energies of the 24 stoichiometrically feasible pathways. The bars indicate the 5% deviations assumed.

ble independent pathways generated via the graph-theoretic method based on P-graphs from the elementary reactions. Note that all feasible pathways give rise to a single overall reaction: $11CO + 19H_2 \leftrightarrow CH_4 + 7H_2O + 2CO_2 + 2C_2H_6 + 2C_2H_4$, as expected. Fig. 3 plots the cumulative activation energies and corresponding 5% deviations of all the feasible pathways listed in Table 2.

3.1. Stoichiometrically feasible pathways

Based on the 26 elementary reactions listed in Table 1, which takes into account carbide, CO-insertion and water-gas shift (WGS) mechanisms (Storsæter et al., 2006), the current graph-theoretic method based on P-graphs has generated 24 stoichiometrically feasible independent pathways (IP_i 's) given in Table 2 in less than 1 s on a PC (Pentium 4, CPU 3.06 GHz and 1G RAM). It is worth noting that every IP_i consists of all the three aforementioned mechanisms except IP_6 , IP_{18} , IP_{19} , and IP_{20} . Specifically, IP_6 only comprises the carbide and WGS mechanisms; and IP_{18} , IP_{19} and IP_{20} , only the CO-insertion and WGS mechanisms.

Table 2

List of computational results of overall independent mechanisms for light hydrocarbons generation through Fischer-Tropsch synthesis.

Designation (IP_i)	Mechanisms
IP_1	$11s_1 + 19s_2 + 7s_3 + 7s_4 + 7s_5 + s_7 + 7s_8 + 7s_9 + 5s_{10} + 5s_{11} + 5s_{12} + 5s_{13} + 2s_{15} + 2s_{16} + 7s_{17} - 3s_{19} - 3s_{20} - 3s_{21} - 3s_{22} + 2s_{23} + 2s_{24} + 2s_{25} + 2s_{26}$
IP_2	$11s_1 + 19s_2 + 7s_3 + 7s_4 + 7s_5 + 3s_6 + s_7 + 7s_8 + 7s_9 + 2s_{10} + 2s_{11} + 2s_{12} + 2s_{13} + 2s_{15} + 2s_{16} + 4s_{17} + 2s_{23} + 2s_{24} + 2s_{25} + 2s_{26}$
IP_3	$11s_1 + 19s_2 + 7s_3 + 7s_4 + 7s_5 + 3s_6 + s_7 + 7s_8 + 7s_9 + 2s_{12} + 2s_{13} + 2s_{15} + 2s_{16} + 4s_{17} - 2s_{18} + 2s_{19} + 2s_{20} + 2s_{21} + 2s_{23} + 2s_{24} + 2s_{25} + 2s_{26}$
IP_4	$11s_1 + 19s_2 + 7s_3 + 7s_4 + 7s_5 + s_7 + 7s_8 + 7s_9 + 5s_{12} + 5s_{13} + 2s_{15} + 2s_{16} + 7s_{17} - 5s_{18} + 2s_{19} + 2s_{20} + 2s_{21} - 3s_{22} + 2s_{23} + 2s_{24} + 2s_{25} + 2s_{26}$
IP_5	$11s_1 + 19s_2 + 7s_3 + 7s_4 + 7s_5 + s_7 + 7s_8 + 7s_9 + 2s_{10} + 2s_{11} + 5s_{12} + 5s_{13} + 2s_{15} + 2s_{16} + 7s_{17} - 3s_{18} - 3s_{22} + 2s_{23} + 2s_{24} + 2s_{25} + 2s_{26}$
IP_6	$11s_1 + 19s_2 + 9s_3 + 9s_4 + 9s_5 + 5s_6 + s_7 + 7s_8 + 7s_9 - 2s_{14} + 2s_{15} + 2s_{16} + 4s_{17} + 2s_{23} + 2s_{24} + 2s_{25} + 2s_{26}$
IP_7	$11s_1 + 19s_2 + 9s_3 + 9s_4 + 9s_5 + s_7 + 7s_8 + 7s_9 + 5s_{12} + 5s_{13} - 2s_{14} + 2s_{15} + 2s_{16} + 9s_{17} - 5s_{18} - 5s_{22} + 2s_{23} + 2s_{24} + 2s_{25} + 2s_{26}$
IP_8	$11s_1 + 19s_2 + 9s_3 + 9s_4 + 9s_5 + 9s_6 + s_7 + 7s_8 + 7s_9 - 4s_{12} - 4s_{13} - 2s_{14} + 2s_{15} + 2s_{16} + 4s_{18} + 4s_{22} + 2s_{23} + 2s_{24} + 2s_{25} + 2s_{26}$
IP_9	$11s_1 + 19s_2 + 7s_3 + 7s_4 + 7s_5 + 7s_6 + s_7 + 7s_8 + 7s_9 + 2s_{10} + 2s_{11} - 2s_{12} - 2s_{13} + 2s_{15} + 2s_{16} + 4s_{18} + 4s_{22} + 2s_{23} + 2s_{24} + 2s_{25} + 2s_{26}$
IP_{10}	$11s_1 + 19s_2 + 7s_3 + 7s_4 + 7s_5 + 7s_6 + s_7 + 7s_8 + 7s_9 - 2s_{10} - 2s_{11} - 2s_{12} - 2s_{13} + 2s_{15} + 2s_{16} + 4s_{19} + 4s_{20} + 4s_{21} + 4s_{22} + 2s_{23} + 2s_{24} + 2s_{25} + 2s_{26}$
IP_{11}	$11s_1 + 19s_2 + 7s_3 + 7s_4 + 7s_5 + 7s_6 + s_7 + 7s_8 + 7s_9 - 2s_{12} - 2s_{13} + 2s_{15} + 2s_{16} + 2s_{18} + 2s_{19} + 2s_{20} + 2s_{21} + 4s_{22} + 2s_{23} + 2s_{24} + 2s_{25} + 2s_{26}$
IP_{12}	$11s_1 + 19s_2 + 7s_3 + 7s_4 + 7s_5 + 5s_6 + s_7 + 7s_8 + 7s_9 + 2s_{10} + 2s_{11} + 2s_{15} + 2s_{16} + 2s_{17} + 2s_{18} + 2s_{22} + 2s_{23} + 2s_{24} + 2s_{25} + 2s_{26}$
IP_{13}	$11s_1 + 19s_2 + 7s_3 + 7s_4 + 7s_5 + 5s_6 + s_7 + 7s_8 + 7s_9 + 2s_{15} + 2s_{16} + 2s_{17} + 2s_{19} + 2s_{20} + 2s_{21} + 2s_{22} + 2s_{23} + 2s_{24} + 2s_{25} + 2s_{26}$
IP_{14}	$11s_1 + 19s_2 - 4s_6 + s_7 + 7s_8 + 7s_9 + 9s_{10} + 9s_{11} + 9s_{12} + 9s_{13} + 7s_{14} + 2s_{15} + 2s_{16} + 4s_{17} + 2s_{23} + 2s_{24} + 2s_{25} + 2s_{26}$
IP_{15}	$11s_1 + 19s_2 - 4s_6 + s_7 + 7s_8 + 7s_9 + 9s_{12} + 9s_{13} + 7s_{14} + 2s_{15} + 2s_{16} + 4s_{17} - 9s_{18} + 9s_{19} + 9s_{20} + 9s_{21} + 2s_{23} + 2s_{24} + 2s_{25} + 2s_{26}$
IP_{16}	$11s_1 + 19s_2 + 5s_6 + s_7 + 7s_8 + 7s_9 + 9s_{10} + 9s_{11} + 7s_{14} + 2s_{15} + 2s_{16} - 5s_{17} + 9s_{18} + 9s_{22} + 2s_{23} + 2s_{24} + 2s_{25} + 2s_{26}$
IP_{17}	$11s_1 + 19s_2 + 5s_6 + s_7 + 7s_8 + 7s_9 + 7s_{14} + 2s_{15} + 2s_{16} - 5s_{17} + 9s_{19} + 9s_{20} + 9s_{21} + 9s_{22} + 2s_{23} + 2s_{24} + 2s_{25} + 2s_{26}$
IP_{18}	$11s_1 + 19s_2 + s_7 + 7s_8 + 7s_9 + 9s_{10} + 9s_{11} + 5s_{12} + 5s_{13} + 7s_{14} + 2s_{15} + 2s_{16} + 4s_{18} + 2s_{22} + 2s_{23} + 2s_{24} + 2s_{25} + 2s_{26}$
IP_{19}	$11s_1 + 19s_2 + s_7 + 7s_8 + 7s_9 + 5s_{10} + 5s_{11} + 5s_{12} + 5s_{13} + 7s_{14} + 2s_{15} + 2s_{16} + 4s_{19} + 4s_{20} + 4s_{21} + 4s_{22} + 2s_{23} + 2s_{24} + 2s_{25} + 2s_{26}$
IP_{20}	$11s_1 + 19s_2 + s_7 + 7s_8 + 7s_9 + 5s_{12} + 5s_{13} + 7s_{14} + 2s_{15} + 2s_{16} - 5s_{18} + 9s_{19} + 9s_{20} + 9s_{21} + 4s_{22} + 2s_{23} + 2s_{24} + 2s_{25} + 2s_{26}$
IP_{21}	$11s_1 + 19s_2 + 4s_3 + 4s_4 + 4s_5 + s_7 + 7s_8 + 7s_9 + 5s_{10} + 5s_{11} + 5s_{12} + 5s_{13} + 3s_{14} + 2s_{15} + 2s_{16} + 4s_{17} + 2s_{23} + 2s_{24} + 2s_{25} + 2s_{26}$
IP_{22}	$11s_1 + 19s_2 + 4s_3 + 4s_4 + 4s_5 + s_7 + 7s_8 + 7s_9 + 5s_{12} + 5s_{13} + 3s_{14} + 2s_{15} + 2s_{16} + 4s_{17} - 5s_{18} + 5s_{19} + 5s_{20} + 5s_{21} + 2s_{23} + 2s_{24} + 2s_{25} + 2s_{26}$
IP_{23}	$11s_1 + 19s_2 + 5s_3 + 5s_4 + 5s_5 + 5s_6 + s_7 + 7s_8 + 7s_9 + 4s_{10} + 4s_{11} + 2s_{14} + 2s_{15} + 2s_{16} + 4s_{18} + 4s_{22} + 2s_{23} + 2s_{24} + 2s_{25} + 2s_{26}$
IP_{24}	$11s_1 + 19s_2 + 5s_3 + 5s_4 + 5s_5 + 5s_6 + s_7 + 7s_8 + 7s_9 + 2s_{14} + 2s_{15} + 2s_{16} + 4s_{19} + 4s_{20} + 4s_{21} + 4s_{22} + 2s_{23} + 2s_{24} + 2s_{25} + 2s_{26}$

3.2. Energetically favorable pathways

Fig. 3 compares the cumulative activation energies of all stoichiometrically feasible pathways listed in Table 2. The cumulative activation energy of IP₁₉ is the lowest while that of IP₇ is the highest among the 24 stoichiometrically feasible IP_i's. This clearly indicates that IP₁₉ is the most energetically favorable, and possibly, it is the dominant pathway. Moreover, the activation energies of IP₁₈ and IP₂₀, which are the second and third lowest, respectively, are close to that of IP₁₉. Note that each of these three pathways consists only of the CO-insertion and WGS mechanisms, as mentioned earlier; thus, it is highly likely that the FTS proceeds through a pathway involving the CO-insertion mechanism rather than the carbide mechanism. This is consistent with that reported in an earlier work (Storsæter et al., 2006), although IP₂₂ might also be plausible because of its overlapping probability distribution with that of IP₁₉.

Among the 26 elementary reactions in Table 1, s_1 through s_{14} are known to constitute the initiation steps (s_1 through s_9 belonging to the carbide mechanism; s_1 , s_2 , and s_7 through s_{14} belonging to the CO insertion mechanism), and s_{17} through s_{26} constitute the chain propagation steps (s_{17} and s_{23} through s_{26} belonging to the carbide mechanism; s_{18} through s_{26} belonging to the CO insertion mechanism). Based on the microkinetic model, Storsæter et al. (2006) have contended that the rate limiting step for initiation is s_{11} ($\text{CHO}^* + \text{H}^* \leftrightarrow \text{CH}_2\text{O}^* + ^*$) while the rate limiting step for chain growth is s_{19} ($\text{CH}_3^* + \text{CO}^* \leftrightarrow \text{CH}_3\text{CO}^* + ^*$). Note that the rate limiting step of any pathway should, in principle, be the one with the greatest activation energy barrier in this pathway. Hence, on the basis of the activation energies listed in Table 1, it is probable that the rate determining step for the initiation is s_{10} ($\text{CO}^* + \text{H}^* \leftrightarrow \text{CHO}^* + ^*$), instead of s_{11} ; while s_{19} and s_{20} are both plausible in IP₁₉.

4. Concluding remarks

The stoichiometrically feasible pathways of FTS have been rigorously and exhaustively identified by resorting to the graph-theoretic method based on P-graphs. A single potentially dominant pathway, comprising only the CO-insertion and WGS mechanisms, has emerged from the judicious analysis of energetics of these stoichiometrically feasible pathways. Moreover, the rate determining steps for the initiation and chain growth have been ascertained. The discrepancy between these rate determining steps and those reported earlier needs to be clarified through further experimental and/or theoretical explorations, such as in situ spectroscopic measurements (Jacobs, Chaney, Patterson, Das, & Davis, 2004), the regression analysis of experimental rate data on the mechanistic models derived from the plausibly dominant pathways, and the calculation of chemisorption energies via the density functional theory (Bligaard et al., 2004).

Acknowledgements

This work was sponsored by National Science Council (Taiwan) under Project NSC-096-2917-I-564-114 and the Hungarian Scientific Research Fund under Project F51227. Professor Scott M. Auerbach at Department of Chemistry, University of Massachusetts-Amherst is gratefully appreciated for valuable discussion.

Appendix A. Supplementary data

Supplementary data associated with this article can be found, in the online version, at doi:10.1016/j.compchemeng.2009.01.003.

References

- Biggs, N. L., Lloyd, E. K., & Wilson, R. J. (1976). *Graph theory*. Oxford, UK: Clarendon, pp. 1736–1936.
- Bligaard, T., Norskov, J. K., Dahl, S., Matthiesen, J., Christensen, C. H., & Sehested, J. (2004). The Bronsted–Evans–Polanyi relation and the volcano curve in heterogeneous catalysis. *Journal of Catalysis*, 224, 206–217.
- Broadbelt, L. J., Stark, S. M., & Klein, M. T. (1994). Computer generated pyrolysis modeling: on-the-fly generation of species, reactions, and rates. *Industrial & Engineering Chemistry Research*, 33, 790–799.
- Callaghan, C., Fishtik, I., Datta, R., Carpenter, M., Chmielewski, M., & Lugo, A. (2003). An improved microkinetic model for the water–gas shift reaction on copper. *Surface Science*, 541, 21–30.
- Dry, M. E., & Hoogendoorn, J. C. (1981). Technology of the Fischer–Tropsch process. *Catalysis Reviews—Science and Engineering*, 23, 265–278.
- Davis, B. H. (2001). Fischer–Tropsch synthesis: Current mechanism and futuristic needs. *Fuel Processing Technology*, 71, 157–166.
- Djéga-Mariadassou, G., & Boudart, M. (2003). Classical kinetics of catalytic reactions. *Journal of Catalysis*, 216, 89–97.
- Fan, L. T., Bertók, B., Friedler, F., & Shafie, S. (2001). Mechanisms of ammonia-synthesis reaction revisited with the aid of a novel graph-theoretic method for determining candidate mechanisms in deriving the rate law of a catalytic reaction. *Hungarian Journal of Industrial Chemistry*, 29, 71–80.
- Fan, L. T., Bertók, B., & Friedler, F. (2002). A graph-theoretic method to identify candidate mechanisms for deriving the rate law of a catalytic reaction. *Computers & Chemistry*, 26, 265–292.
- Fan, L. T., Shafie, S., Bertók, B., Friedler, F., Lee, D. Y., Seo, H., et al. (2005). Graph-theoretic approach for identifying catalytic or metabolic pathways. *Journal of the Chinese Institute of Engineers*, 28, 1021–1037.
- Fan, L. T., Lin, Y.-C., Shafie, S., Hohn, K. L., Bertók, B., & Friedler, F. (2007). Comment on: An improved microkinetic model for the water–gas shift reaction on copper [Surf. Sci. 541 (2003) 21–30]. *Surface Science*, 601, 2401–2405.
- Fan, L. T., Lin, Y.-C., Shafie, S., Hohn, K. L., Bertók, B., & Friedler, F. (2008). Graph-theoretic and energetic exploration of catalytic pathways of the water–gas shift reaction. *Journal of the Chinese Institute of Chemical Engineers*, 39, 467–473.
- Fischer, F., & Tropsch, H. (1926a). The direct synthesis of petroleum hydrocarbons with standard pressure. (First report.). *Berichte Der Deutschen Chemischen Gesellschaft*, 59, 830–831.
- Fischer, F., & Tropsch, H. (1926b). The direct synthesis of petroleum hydrocarbons with standard pressure. (Second report.). *Berichte Der Deutschen Chemischen Gesellschaft*, 59, 832–836.
- Fischer, F., & Tropsch, H. (1926c). *Brennstoff-Chemie*, 7, 97.
- Fishtik, I., & Datta, R. (2002). A UBI-QEP microkinetic model for the water–gas shift reaction on Cu(111). *Surface Science*, 512, 229–254.
- Friedler, F., Tarján, K., Huang, Y. W., & Fan, L. T. (1992). Graph-theoretic approach to process synthesis: Axioms and theorems. *Chemical Engineering Science*, 47, 1973–1988.
- Friedler, F., Tarján, K., Huang, Y. W., & Fan, L. T. (1993). Graph-theoretic approach to process synthesis: Polynomial algorithm for maximal structure generation. *Computers & Chemical Engineering*, 17, 929–942.
- Friedler, F., Varga, J. B., & Fan, L. T. (1995). Decision-mapping: A tool for consistent and complete decisions in process synthesis. *Chemical Engineering Science*, 50, 1755–1768.
- Imreh, B., Friedler, F., & Fan, L. T. (1996). An algorithm for improving the bounding procedure in solving process network synthesis by a branch-and-bound method. In I. Bomze, T. Csendes, R. Horst, & P. Pardalos (Eds.), *Nonconvex optimization and its applications: Developments in global optimization* (pp. 315–348). Dordrecht: Kluwer Academic Publishers.
- Jacobs, G., Chaney, J. A., Patterson, P. M., Das, T. K., & Davis, B. H. (2004). Fischer–Tropsch synthesis: Study of the promotion of Re on the reduction property of Co/Al₂O₃ catalysts by in situ EXAFS/XANES of Co K and Re L-III edges and XPS. *Applied Catalysis A: General*, 264, 203–212.
- Khodakov, A. Y., Chu, W., & Fongarland, P. (2007). Advances in the development of novel cobalt Fischer–Tropsch catalysts for synthesis of long-chain hydrocarbons and clean fuels. *Chemical Reviews*, 107, 1692–1744.
- Klinke, D. J., & Broadbelt, L. J. (1997). Mechanism reduction during computer generation of compact reaction models. *AIChE Journal*, 43, 1828–1837.
- Lee, D. Y., Fan, L. T., Park, S., Lee, S. Y., Shafie, S., Bertók, B., et al. (2005). Complementary identification of multiple flux distributions and multiple metabolic pathways. *Metabolic Engineering*, 7, 182–200.
- Li, C., Henry, C. S., Jankowski, M. D., Ionita, J. A., Hatzimanikatis, V., & Broadbelt, L. J. (2004). Computational discovery of biochemical routes to specialty chemicals. *Chemical Engineering Science*, 59, 5051–5060.
- Lin, Y.-C., Fan, L. T., Shafie, S., Hohn, K. L., Bertók, B., & Friedler, F. (2008). Catalytic pathways identification for partial oxidation of methanol on copper–zinc catalysts: $\text{CH}_3\text{OH} + 1/2\text{O}_2 \leftrightarrow \text{CO}_2 + 2\text{H}_2$. *Industrial & Engineering Chemistry Research*, 47, 2523–2527.
- Lin, Y.-C., & Huber, G. W. (2009). The critical role of heterogeneous catalysis in lignocellulosic biomass conversion. *Energy & Environmental Science*, 2, 68–80.
- Lox, E. S., & Froment, G. F. (1993a). Kinetics of the Fischer–Tropsch reaction on a precipitated promoted iron catalyst. 1. Experimental procedure and results. *Industrial & Engineering Chemistry Research*, 32, 61–70.
- Lox, E. S., & Froment, G. F. (1993b). Kinetics of the Fischer–Tropsch reaction on a precipitated promoted iron catalyst. 2. Kinetic modelling. *Industrial & Engineering Chemistry Research*, 32, 71–82.

- Matheu, D. M., Lada, T. A., Green, W. H., Jr., Dean, A. M., & Grenda, J. M. (2001). Rate-based screening of pressure-dependent reaction networks. *Computer Physics Communications*, *138*, 237–249.
- Matheu, D. M., Green, W. H., Jr., & Grenda, J. M. (2003). Capturing pressure-dependence in automated mechanism generation: Reactions through cycloalkyl intermediates. *International Journal of Chemical Kinetics*, *35*, 95–119.
- Matheu, D. M., Dean, A. M., Grenda, J. M., & Green, W. H., Jr. (2003). Mechanism generation with integrated pressure dependence: A new model for methane pyrolysis. *Journal of Physical Chemistry A*, *107*, 8552–8565.
- Pichler, H., & Schulz, H. (1970). Recent results in synthesis of hydrocarbons from CO and H₂. *Chemie Ingenieur Technik*, *42*, 1162–1174.
- Rados, N., Al-Dahhan, M. H., & Dudukovic, M. P. (2003). Modeling of the Fischer–Tropsch synthesis in slurry bubble column reactors. *Catalysis Today*, *79–80*, 211–218.
- Seo, H., Lee, D. Y., Park, S., Fan, L. T., Shafie, S., Bertók, B., et al. (2001). Graph-theoretical identification of pathways for biochemical reactions. *Biotechnology Letters*, *23*, 1551–1557.
- Storsæter, S., Chen, D., & Holmen, A. (2006). Microkinetic modelling of the formation of C₁ and C₂ products in the Fischer–Tropsch synthesis over cobalt catalysts. *Surface Science*, *600*, 2051–2063.
- Van der Laan, G. P., & Beenackers, A. A. C. M. (1999). Kinetics and selectivity of the Fischer–Tropsch synthesis: A literature review. *Catalysis Reviews—Science and Engineering*, *41*, 255–318.
- Vilekar, S. A., Fishtik, I., & Datta, R. (2007). Topological analysis of catalytic reaction networks: Methanol decomposition on Pt(1 1 1). *Journal of Catalysis*, *252*, 258–270.